

Research

Enhancing physico-mechanical properties and thermal stability of geopolymer composites through nano-material incorporation

Hisham M.Khater¹ · Mahmoud Gharieb²

Received: 11 October 2023 / Accepted: 26 March 2024

Published online: 08 April 2024

© The Author(s) 2024 [OPEN](#)

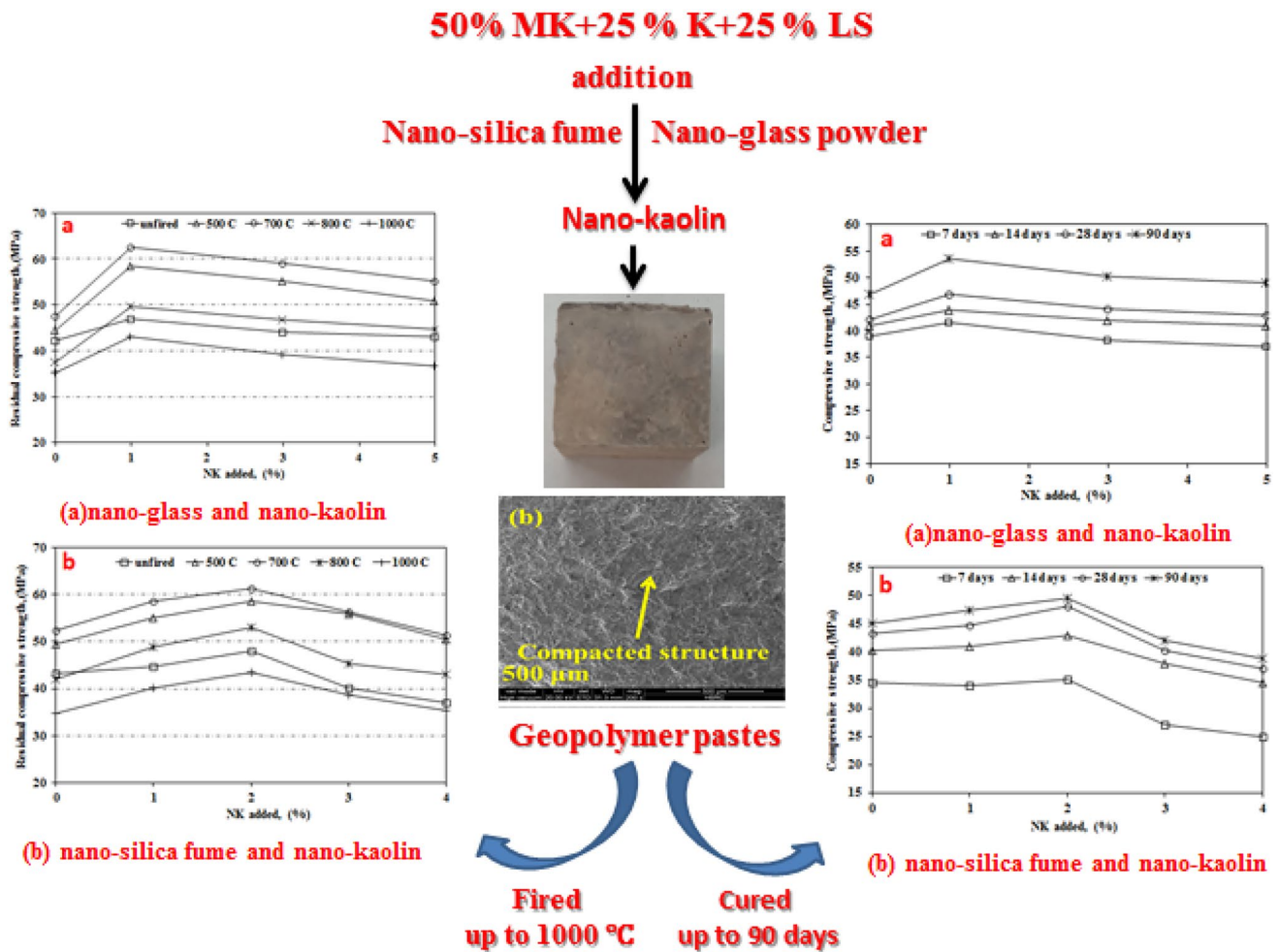
Abstract

Influence of various types of nano powder on the physico-mechanical properties of geopolymer materials has been studied, in addition to studying their firing stability up to 1000 °C. Alumino–silicate materials used are kaolin, fired kaolin and lime stone. Materials prepared at water/binder ratios of 0.40; whereas the used equal volume of activator 5 M sodium hydroxide with liquid sodium silicate. Nano-kaolin admixed with Nano-powder as a partial replacement from metakaolin material. The control mixes incorporating either 7% Nano-glass or 5% Nano-silica fume. Nano-kaolin was partially replaced Nano-glass powder and Nano-silica fume. It is possible to use the mixes containing limestone and nano materials to solve the problem of using heat curing, thermal energy consumption and pollution by reducing the MK used for MK-geopolymer cement. Results indicated an enhancement in the physico-mechanical properties of mix incorporating 1: 6% and 2:3% of NK:N-glass and NK:N-silica fume, respectively. Firing of hardened geopolymer resulted in high thermal resistance up to 700 °C then exposed to decrease up to 1000 °C. However, no micro-cracks were noticed up to 800 °C for all samples as recorded by visual examination of the fired samples, while micro-cracks were recorded for hardened composites at 1000 °C.

✉ Hisham M.Khater, Hkhater4@yahoo.com | ¹Raw Building Materials Technology and Processing Research Institute, Housing and Building National Research Center (HBNRC), 87 El-Tahreer St., Dokki, Giza, P.O. Box 11511, Cairo, Egypt. ²Raw Building Materials Technology and Processing Research Institute, Housing and Building National Research Center (HBNRC), 87 El-Tahreer St., Dokki, Giza, P.O. Box 11511, Cairo, Egypt.



Graphical Abstract



Highlights

1. Studying the effect of nanomaterial on the physicomechanical properties of the formed composites.
2. Examining the thermal stability of the formed composites up to 1000 °C.
3. Producing geopolymer composites with reduced thermal energy consumption.

Keywords Nano- glass · Geopolymer · Microstructure · Compressive strength · Thermal stability

1 Introduction

Nanotechnology has proven in recent years that it is not only a science limited to laboratory research, as it has been highly relied upon many areas (coating, polymer, fibers and electronics) that have been developed. In the modern era, nanotechnology must be completely relied upon various industries, because of its many characteristics, the most important of which is that it reduces costs, gives better quality, and reduces the amount of environmental pollution [1, 2].

When material particles are converted from normal size to nanoscale, this change in size improves their physico-mechanical and chemical properties [3, 4]; highlighted the nanotechnology of materials in the field of construction that

gives unique physical and chemical properties compared to traditional materials. Moreover, the rapid development in the field of nano-science of materials has provided construction companies and civil engineers with a new window of understanding in traditional building materials, such as cement, chemical and mineral additives or steel, allowing us to enhance their physical and mechanical properties, reduce energy consumption, and extend their lifespan with low cost [5].

Researchers have tried various methods to introduce nanomaterials into composite materials to improve their characteristics and structural performance. The impacts of different nanomaterials on the fresh, hardened properties and microstructure features of conventional concrete, geopolymer concrete, cement pastes were studied, analyses, and discussed in this studied. Different nanomaterials have different characteristics, improving one or more properties of composite materials with the small dosage of NMs ranging from 0 to 3%. The result of this study show that adding NMs to high-performance composites makes them stronger, more durable, and have a better microstructure property and it shows NMs are the future in the construction material industry [6, 7].

Khater et al., [8], also studied the effect of adding different percentages of nano-silica materials from 0 to 1.5% on the physical and mechanical properties of alkali activated slag geopolymer. The results showed that the physical and mechanical properties improved with the increase in the percentage of nano silica. The study also showed that with the increase in the percentage of nano silica, the thermal properties as well as the thermal insulation property improved. Kuo et al., [9] showed that the mechanical properties of compressive strength and flexural strengths of cement mortar improve with the addition of nanoparticles of silica oxide SiO_2 and iron oxide Fe_2O_3 . When adding nanoparticles to cement materials, it increases the hydration process, and this is due to many factors, the most important of which is its high activity, in addition to the process of uniform dispersion in the cement paste, where nanoparticles fill the pores of the cement paste, which leads to improvement, mechanical properties and microstructure of the cement paste [10–14] also studied the influence of the addition of different ratios of Nano-silica from 0% up to 3% on physicochemical and morphological characteristics of Geopolymer materials. Results indicated that the Geopolymer mixes incorporating 2.5% nano-silica give the highest compressive strength values at early ages than those of the control one, with the lowest percentage of water absorption. Khater and Abd el Gawwad [15] also depicted the potential effect of Nano-kaolin on alkaline activation of slag—metakaolin (AAs) binder for preparation of eco-friendly materials (40:60 wt. %). Results indicate that the geopolymer mixes containing 5% Nano-kaolin give the highest physico-mechanical and microstructural characteristics, while further increasing the Nano-kaolin by more than 5% resulted in agglomeration and strength decrease.

Nanoparticles may exhibit size-related characteristics that differ from those observed in bulk materials. They represent the connection between such bulk materials and molecular structures. At the nano-scale, the ratios of atoms at the surface of material become significant providing special properties, e.g. gold nanoparticles melt at 300 °C in comparison with the gold slabs (1064 °C) Buffat and Burrel [16]. When nano-particles (typically SiO_2 , TiO_2 , etc.) are added into cement-based materials, a series of chemical bond connection between the nano-particles and hydration products of cement will be produced, and the nano-particles may become crystal nucleus of the calcium silicate hydrate (C–S–H) gel, in addition these nanoparticles work also as nano filler. They densify the cement paste microstructure by filling the pores between the cement grains. After that, the whole system will change into a dense network structure with the nano-particles as the cores, which will refine the microstructure of cement-based materials effectively [17–20]. However, the complex production process and high cost of these nano-particles obstructs the application of such materials in the cement-based materials widely. Therefore, new nano-particles alternative to the traditional nano materials with high performance, low cost and simple producing process are essential for the sustainable development of the construction industry.

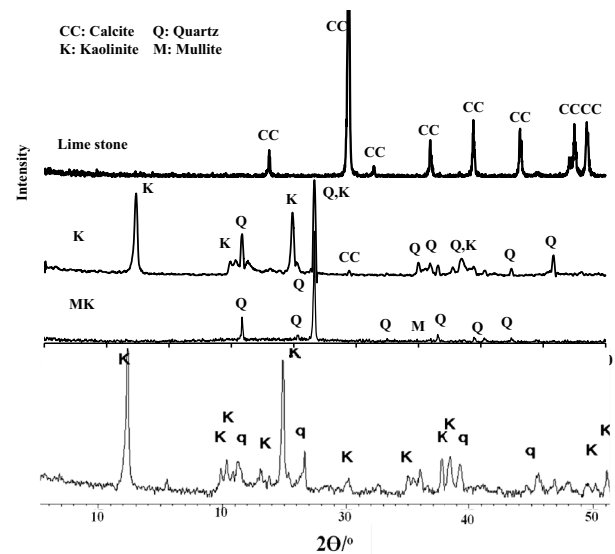
New nano-metric SCM, micrometric waste glass powder, a high amorphous silica content material (70 to 80 wt.%), is vaporized and nucleated into spheroidized glass powder (SGP) using the technology of induction thermal plasma torch, a process comparable to the production of silica fume (SF). This technology has previously demonstrated its ability to vaporize and nucleate waste glass into glass nanoparticles [21]. Where in SGP were studied for their reactivity in cement pastes and mortars and compared to finely ball-mill ground glass powder (GP) and SF. This paper treats the characterization of the materials used and the results regarding the reactivity, the polymerization of the C–S–H chain and compressive strength development when SGP, GP and SF are introduced as a partial replacement of OPC in cement pastes and mortars.

The main objective of this research is to study the effect of Nano materials powder (Nano-kaolin- Nano- glass- Nano-silica fume) on the physical, mechanical and microstructure of geopolymer materials produced from various precursors of aluminosilicates that produce unconventional support materials that can have high potential to be used in high temperature environment, where the stability against high thermal temperature for the hardened mixes will be also monitored. Testing of the resulting geopolymer product is studied using TGA/DTG, compressive strength and bulk

Table 1 Chemical composition of starting materials

| Oxide content (%) | SiO ₂ | Al ₂ O ₃ | Fe ₂ O ₃ | CaO | MgO | SO ₃ | K ₂ O | Na ₂ O | TiO ₂ | MnO | P ₂ O ₅ | Cl ⁻ | BaO | L.O.I | Total |
|---|------------------|--------------------------------|--------------------------------|-------|------|-----------------|------------------|-------------------|------------------|------|-------------------------------|-----------------|------|-------|-------|
| Kaolin (M. East) | 49.86 | 34.10 | 0.30 | 0.09 | 0.26 | 0.59 | 0.02 | 0.03 | 0.88 | 0.00 | 0.35 | 0.00 | 0.00 | 13.44 | 99.92 |
| Kaolin south sinai | 50.10 | 31.46 | 1.42 | 0.31 | 0.19 | 0.14 | 0.08 | 0.12 | 2.67 | 0.00 | 0.14 | 0.07 | 0.00 | 13.01 | 99.81 |
| MK (fired kaolin at 750 degree for 2 h) | 62.37 | 31.60 | 1.47 | 0.26 | 0.01 | 0.01 | 0.15 | 0.12 | 2.60 | 0.00 | 0.01 | 0.03 | 0.00 | 1.16 | 99.86 |
| Limestone | 0.52 | 0.18 | 0.04 | 55.86 | 0.15 | 0.20 | 0.01 | 0.22 | 0.00 | 0.00 | 0.12 | 0.06 | 0.00 | 42.60 | 99.96 |
| Nano-glass powder | 70.25 | 0.88 | 0.21 | 11.90 | 3.42 | 0.41 | 0.09 | 9.99 | 0.06 | 0.00 | 0.01 | 0.09 | 0.01 | 2.63 | 99.95 |
| Nano-silica fume powder | 94.72 | 0.02 | 1.28 | 0.03 | 0.01 | 0.28 | 0.15 | 0.02 | 0.00 | 0.00 | 3.28 | 0.00 | 0.00 | 0.00 | 99.79 |
| Nano-kaolin | 57.53 | 38.63 | 0.35 | 0.11 | 0.30 | 0.01 | 0.03 | 0.56 | 1.02 | 0.41 | 0.93 | 0.00 | 0.00 | 0.00 | 99.88 |

%, Mass

Fig. 1 X-Ray diffraction of the used raw materials

density testing, as well as SEM and visual examination of the fired samples are conducted on pastes of Geopolymer based sample, to elaborate the optimum mixing ratio between NK and each of N-glass and N-SF and the effect of firing temperatures on both matrices.

2 Experimental procedures

2.1 Materials

Binder used in this investigation are high purity kaolinite material imported from Middle East Company, Egypt and kaolin collected from El-Dehesa, South Sinai, Egypt; in addition to powder limestone. Sodium hydroxide (NaOH) in the form of pellets with a purity of 99 % used as alkali activators, obtained from SHIDO Co., Egypt. Commercial sodium silicate used also as an additional activator, an equal volume of 5M sodium hydroxide and liquid sodium silicate was used.

Table 1 showed the chemical compositions of the raw materials, while the mineralogical characterization of the raw materials was done using X-ray diffraction analysis in powder form in Fig. 1. To convert kaolin to metakaolin, kaolin was heat treated at about 800 °C for 2 h at a heating rate of 5 °C/min, to produce metakaolin (MK) [22–24]. Nano-glass powders as well as Nano-silica fume used in this research are a synthetic product with spherical particles in the range of 35–125 nanometers synthesized by dry grinding of aforementioned nano materials for 8 h. While, nano-kaolin is synthesized by firing ultra-fine kaolin at (800 °C) for 2 h with a heating rate of 5 °C, while its size is in the range 35–90 nm. The chemical

analysis showed that it consists mainly of silica and alumina oxides as major content. The physical properties of nano-glass powder are given in Table 2. Transmission Electron Microscopy (TEM) for magnification up to 60,000 by used type JEOL-JEM-1230 to test the particle size of nano-glass used as reflected in Fig. 2.

2.2 Dispersion of nano materials

Nano materials were subjected for sonication using a Fritish 450 Sonifier Analog Cell Distributor for 15 min Collins et al. [25]. Super- plasticizer type (G) used for Nano-powder dispersion Senff et al. [26]. Nano-materials were admixed with various ratios as tabulated in Table 2.

2.3 Geopolymerization and curing

Due to the high surface area of nano-particles, it is difficult to disperse them uniformly if they are spontaneously added to the mixture; therefore, the mixing procedure was carried out as follows:

First, the nano-materials are added with 50% of the mixing water and stirred using a magnetic stirrer for 15 min until the nano-materials are homogenized with the mixing water. Second, the binders are mixed with the other part of mixing water and alkaline activated solution manually for 10 min, then using a rotary mixer and mixed for 5 min at a medium speed (80 rpm). Third, the superplasticizer Glenium Ace-30 of (type G) is added, then the nano-silica material that was prepared in the first step is added, then stirred with the mixture at a high speed for an additional 90 s.

All mixes involved the addition of 20% of 5 M NaOH of dry mixes as well as 20% sodium silicate of the dry mix Shilar et al. [6, 7, 27, 28]. The Water-binder material ratio (w/b) depending on the type and amount of nano content as indicated in the Table 2. Pour the dough mixture into cube-shaped molds (25 × 25 × 25 mm), vibrated for compaction and sealed with a lid to reduce any loss of evaporated water. The samples were left to cure at room temperature 23 °C for 24 h, then the molds were removed, and the samples were then left to be treated with water under room temperature [29–31]. At the end of the curing system, compressive strength measurements were taken at different times. After 28 days of curing, samples were stopped for hydration by drying at (105 °C for 24 h.), and then exposed to firing from 500 up to 1000 °C for 2 h with a heating rate of 5 °C/min.

2.4 Methods of investigation

Chemical analysis of the raw materials was carried out using Axios (PW4400) WD-XRF Sequential Spectrometer. The selected samples were prepared and tested using XRD, TGA/DTG, and SEM. XRD analysis was recorded on a (Philips PW 1050/70) Diffractometer using a Cu-K α source with a post sample K α filter. XRD patterns were collected from (0° to 50° 2 θ step size 0.02° 2 θ and speed 0.4°/min). Thermogravimetric analysis (TGA/DTG) was implemented with the help of a thermal analyzer. The sample in the form of powder was put in a platinum crucible then exposed to (1000 °C with a heating rate of 20 °C/min) in a nitrogen atmosphere. Compressive strength tests were carried out using two tones German Brűf pressing machine determine according to ASTM C109 M-12 [32]. Particle size analysis was done using a laser scattering particle size distribution analyzer (Horiba LA-950, Kyoto, Japan) [33, 34].

Bulk density of the geopolymers mixes was calculated using the formulae [35–37]:

$$\text{Bulk Density} = [W / (W_W - W_A)]$$

where: W, Weight of geopolymer specimen; W_W , Weight of suspended geopolymer specimen in water; and W_A , Weight of soaked geopolymer specimen suspended in air.

Strength change factor of the hardened samples was calculated according to the following equation [38–40]:

$$\text{SCF} = 100 * (F_i - F_f) / F_i$$

Where, F_i is the 28 days compressive strength of the unfired sample, while F_f is the compressive strength of the fired sample at the specified temperature.

Transmission Electronic Microscopic (TEM) type JEOL-JEM-1230, where the sample is magnification up to 60,000 it was to measure the particle size of the nano. The morphology and microstructure of hardened geopolymer composites was examined by [SEM] equipped with EDX. DT-50 m, samples were prepared by plating them with gold before imaging.

Table 2 Composition of the geopolymers mixes

| Mix | Kaolin M.E, % | MK, % | Lime stone, % | Nano-glass, % | Nano-silica fume, % | Nano-kaolin, % | NaOH (5 M), % | Na ₂ SiO ₃ , % | SP, % | T. Water/binder | Total M ₂ O/Al ₂ O ₃ | SiO ₂ /Al ₂ O ₃ | SiO ₂ /(Al ₂ O ₃ +M ₂ O) | Total M ₂ O/SiO ₂ |
|------|---------------|-------|---------------|---------------|---------------------|----------------|---------------|--------------------------------------|-------|-----------------|---|--|--|---|
| NG0 | 25 | 43 | 25 | 7 | - | 0 | 20 | 20 | 1.6 | 0.40 | 0.78 | 2.28 | 2.18 | 0.20 |
| NG1 | 25 | 43 | 25 | 6 | - | 1 | 20 | 20 | 1.0 | 0.40 | 0.76 | 2.24 | 2.17 | 0.20 |
| NG3 | 25 | 43 | 25 | 4 | - | 3 | 20 | 20 | 1.2 | 0.40 | 0.72 | 2.16 | 2.13 | 0.20 |
| NG5 | 25 | 43 | 25 | 2 | - | 5 | 20 | 20 | 1.4 | 0.40 | 0.68 | 2.08 | 2.10 | 0.19 |
| NSF0 | 25 | 45 | 25 | - | 5 | 0 | 20 | 20 | 1.6 | 0.40 | 0.70 | 2.27 | 2.27 | 0.18 |
| NSF1 | 25 | 45 | 25 | - | 4 | 1 | 20 | 20 | 1.0 | 0.40 | 0.69 | 2.22 | 2.23 | 0.18 |
| NSF3 | 25 | 45 | 25 | - | 3 | 2 | 20 | 20 | 1.2 | 0.40 | 0.68 | 2.16 | 2.19 | 0.19 |
| NSF5 | 25 | 45 | 25 | - | 2 | 3 | 20 | 20 | 1.4 | 0.40 | 0.67 | 2.11 | 2.15 | 0.19 |
| NSF7 | 25 | 45 | 25 | - | 1 | 4 | 20 | 20 | 1.6 | 0.40 | 0.66 | 2.07 | 2.12 | 0.19 |

% Mass

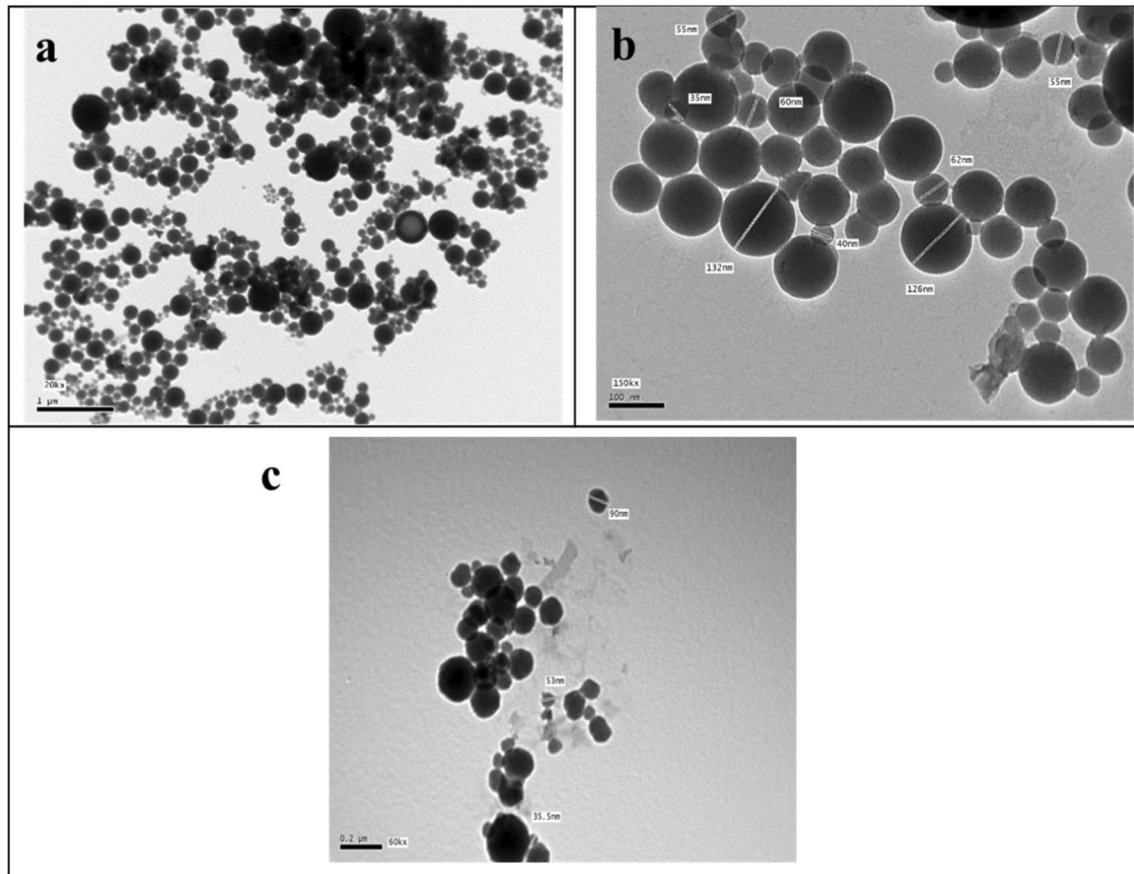


Fig. 2 TEM of the used materials: **a** Nano-glass waste powder, **b** Nanosilica fume, **c** Nano-kaolin

Bonding characteristics of the geopolymer specimens were analyzed using Fourier transformed infrared spectrometer [FTIR]. The test sample was uniformly milled with KBr in a weight ratio of KBr: sample = 200:1, the mixture, 0.20 g was pressed onto a 13 mm diameter disc for analysis at 8 t/cm², the wave number was from 400 to 4000 cm⁻¹ [41–44].

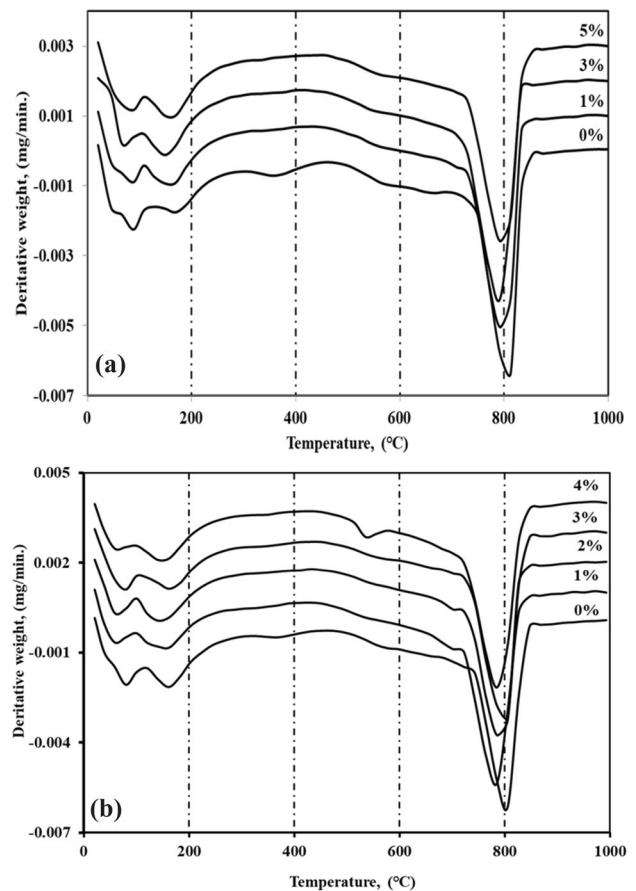
3 Results and discussion

3.1 Nano- materials effect on geopolymer composite properties

3.1.1 Thermo-gravimetric analysis (TGA/DTG)

Figures 3a, b, 4a, b shows the TGA/DTG curves of specimens enhanced with mixed ratio of nano-glass and nano-kaolin (NG0, NG1, NG3, NG5) and specimens enhanced with mixed ratio of nano-silica fume and nano-kaolin (NSF0, NSF1, NSF2, NSF3, NSF4). From a general view, all samples show a weight loss at a temperature below 300 °C followed by a weight loss at a temperature ~ 800 °C. The first one which is due to the decomposition of free water as well as the coexistence between (N–A–S–H) and (C–S–H) gel [45, 46]. The results reveal that, the intensity of peaks below 300 °C increases with mixed nano-kaolin with nano-glass and nano-silica fume in all geopolymer mixes compared to the control mix, whereas the weight losses are 4.96%, 5.79%, 5.56% and 5.25% for NG0, NG1, NG3 and NG5, respectively. While, the weight losses are 4.66%, 5.30%, 5.62%, 5.09 and 4.83% for NSF0, NSF1, NSF2, NSF3 and NSF4, respectively. The samples of NG1 and NSF2 exhibits the highest weight loss before (200 °C) (Fig. 5), confirming its highest strength as a results of dehydration of NSH and CSH formed in the matrix. The second one is located at a temperature (~ 800 °C) this loss is related to the decomposition of carbonate phases (calcium/sodium carbonates) Ismail et al. [47].

Fig. 3 DTG of alkali activated specimens enhanced with mixed ratio of nano materials, **a** nano-glass and nano-kaolin, **b** nano-silica fume and nano-kaolin



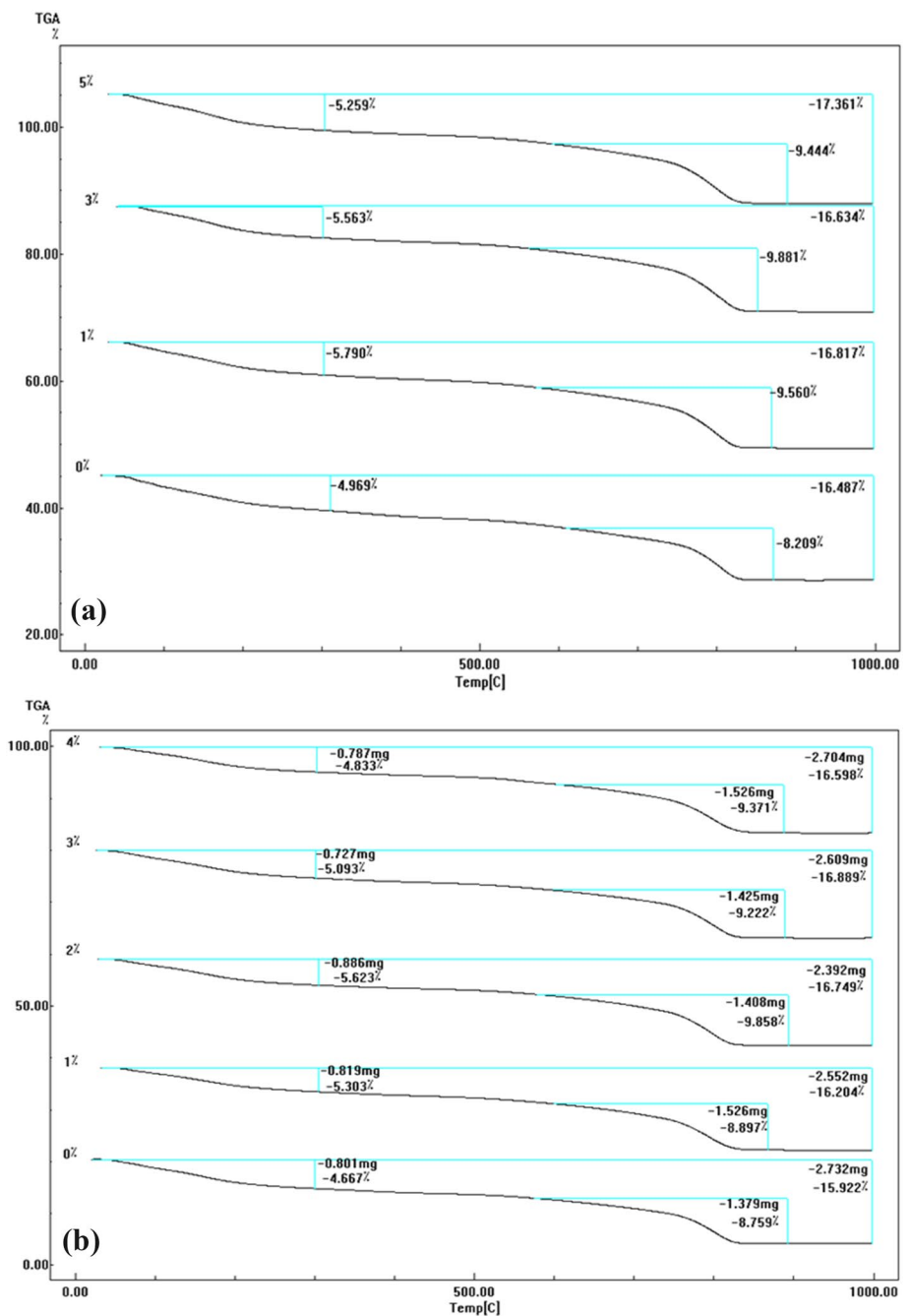
3.1.2 Compressive strength

The variations in strength as a function of nano-kaolin contents in various series of nano-glass and nano-silica fume geopolymers cured at 7, 14, 28 and 90 days are illustrated in Fig. 5a, b. For all curing times and replacement levels of nano-kaolin in alkali-activated geopolymer mixes made with nano-glass and nano-silica fume, the compressive strength of specimens' raises, indicating the continued acceleration of geopolymerization process to produce more hydration products of (N–A–S–H and C–S–H gel) which deposit in the available open pore spaces to form dense and compacted microstructure of the geopolymer matrix.

Figure 5a explains the compressive strength values of the geopolymer samples that increases with replaced nano-glass with nano-kaolin up to 1 wt. % then it decreases with further increasing nano-kaolin at all curing time up to 90 days but still more than those of control mix. The incorporation of 6% nano-glass with 1% nano-kaolin (NG1) gives the highest compressive strength compared with the other mixes containing nano-kaolin as well as its leads to an increase in the strength values at the age of 7, 14, 28 and 90 days by an average of 6.4%, 7.3%, 11.6% and 14% compared with that of the NG0, respectively.

Figure 5b show the compressive strength values of the geopolymer samples that increase with replaced nano-silica fume with nano-kaolin up to 2 wt. % then it decreases with further increase in nano-kaolin at all curing time up to 90 days. Incorporation of 3% nano-silica fume with 2% nano-kaolin (NSF2) gives the highest compressive strength compared with the other mixes and increases the compressive strength by about 1.3%, 6.7%, 11.4% and 10.2% at the ages of 7, 14, 28 and 90 days compared with that of NSF0, respectively. The results indicate that, with the additional increase of nano-kaolin to nano-silica fume a weakness in the physicomechanical properties of the geopolymer pastes, as it works to impede the diffusion of the geopolymer chain. The improvement of compressive strength values with adding nano-kaolin to nano-glass and nano-silica fume Fig. 5a, b, is due to, the dual properties of nano-kaolin, physical (filler) effect and chemical (pozzolanic) effects, its leads to the accumulation of more hydration products of sodium aluminosilicates hydrate and calcium aluminosilicates hydrate along with calcium silicate gel, resulting in the formation of a homogeneous and denser microstructure.

Fig. 4 Thermogravimetric analysis of alkali activated specimens enhanced with mixed ratio of nano materials, **a** nano-glass and nano-kaolin, **b** nano-silica fume and nano-kaolin



3.1.3 Bulk density investigation

Figure 6a, b show the bulk density of geopolymer pastes having various ratios of nano-kaolin in various series of nano-glass and nano-silica fume geopolymers cured at 7, 14, 28 and 90 days. The results indicate that, the bulk density of all specimens' increases with hydration time up to 90 days. This is mainly due to the improvement of the geopolymerization process with processing time and the formation of excessive amounts of geopolymerization products which accumulate within the open pore system of the hardening pastes resulting in an increase in the bulk density. Figure 6a shows that the density of the geopolymer samples made with nano-glass increased when the nano-kaolin incorporation increased up to 1% then it decreases with increasing nano-kaolin content at all curing time up to 90 days but still more than those of control mix.

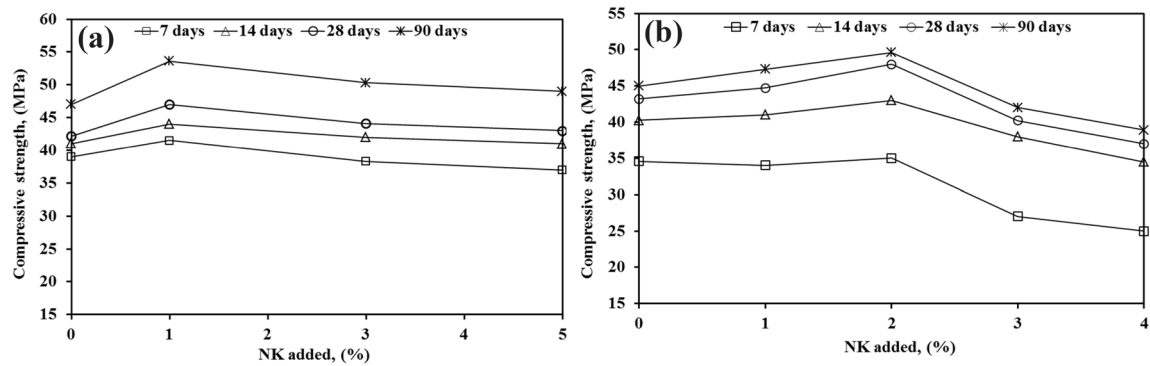


Fig. 5 Compressive strength of alkali activated specimens enhanced with mixed ratio of nano materials, **a** nano-glass and nano-kaolin, **b** nano-silica fume and nano-kaolin

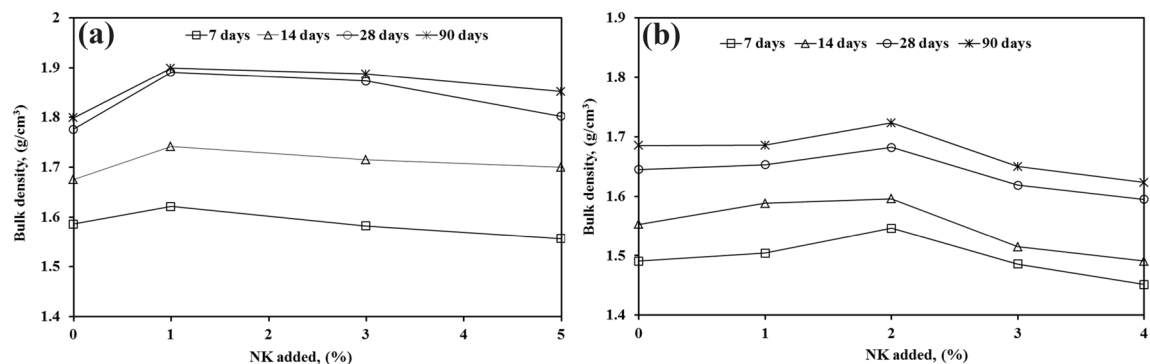


Fig. 6 Bulk density of alkali activated specimens enhanced with mixed ratio of nano materials, **a** nano-glass and nano-kaolin, **b** nano-silica fume and nano-kaolin

Figure 6b show the bulk density of the geopolymer samples that increase with replaced nano-silica fume with nano-kaolin up to 2 wt. % then it decreases with increasing nano-kaolin content at all curing time up to 90 days. As it had a negative effect, which can be attributed to the agglomeration of non-reactive nanoparticles. Incorporation of 3% nano-silica fume with 2% nano-kaolin (NSF2) gives the highest density compared with the other mixes. The improvement of density values with adding nano-kaolin to nano-glass and nano-silica fume Fig. 6a, b which leads to improved compressive strength, is due to, the dual properties of nano-kaolin, physical (filler) effect and chemical (pozzolanic) effects, it leads to the accumulation of more hydration products of sodium aluminosilicates hydrate and calcium aluminosilicates hydrate along with calcium silicate gel, resulting in the formation of a homogeneous and denser microstructure.

3.1.3.1 Scanning electron microscopy (SEM) Figure 7 show the scanning electron micrographs of geopolymer mixes having different ratios of NK at 28 days of curing. The micrograph of the control geopolymer mix appears the porous matrix formation with the spreading of many pores with various sizes within the matrix (Fig. 7a). Using 1% NK results in an enhancement for the matrix morphology and filling most of the formed pores where it acts as nucleation sites for accumulation [48, 49] of the geopolymer constituents leading to the formation of dense and compact structure (Fig. 7b). Increasing NK to 2% leads to formation of agglomerates from NK and N-glass forming heterogeneous structure having many wide pores between the matrix binder and so hinder the formation of the geopolymer network as indicated from the micrograph (7C) Khater [50].

On examining the microstructure of 28 days of N-silica fume matrices having various ratios of NK (Fig. 8); the same behavior is noticed where control mix have many wide pores spreads forming heterogeneous structure with few point of interaction between their binding constituents (Fig. 8a). Using 2% NK results in an enhancement for the matrix morphology and filling most of the formed pores where it acts as nucleation sites for accumulation [48, 49] of the geopolymer constituents leading to the formation of three dimensional network (Fig. 8b). Increasing NK to 3% leads to formation of

Fig. 7 SEM images of alkali activated specimens enhanced with mixed ratio of nano materials of nano-glass and **a** 0, **b** 1, **c** 3 nano-kaolin

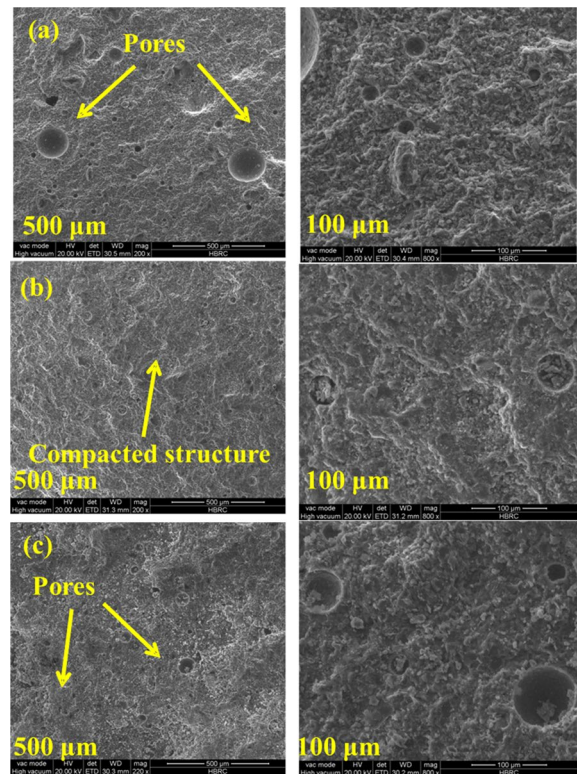
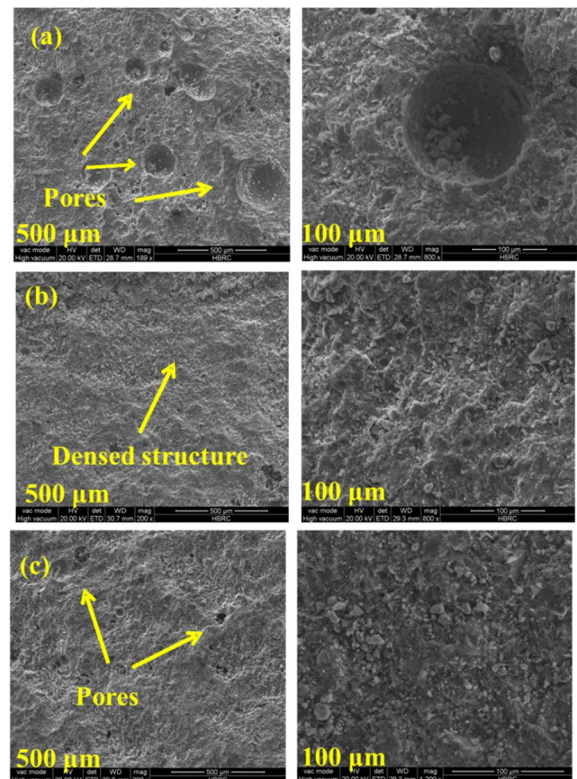


Fig. 8 SEM images of alkali activated specimens enhanced with mixed ratio of nano materials of nano-silica fume and **a** 0, **b** 2, **c** 3 nano-kaolin.



agglomerates from NK and N-glass forming wide voids between the matrix binder and so hinder the formation of the geopolymer network as indicated from the micrograph (Fig. 8C) [51, 52].

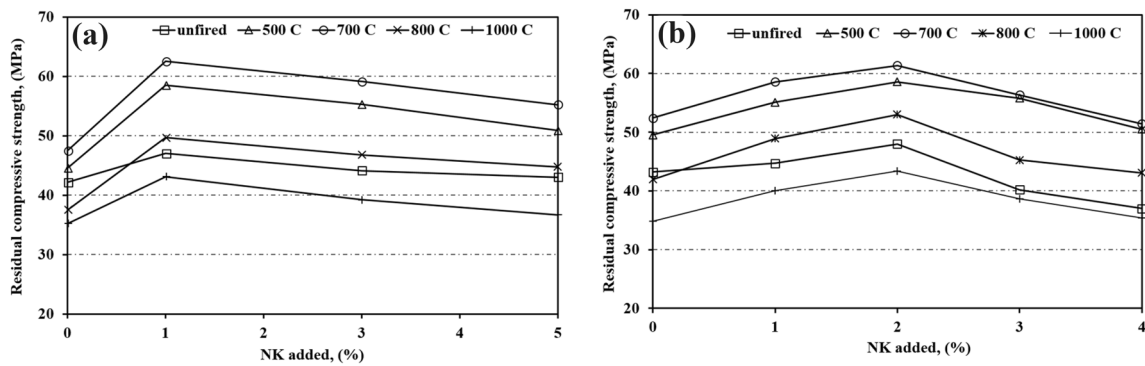


Fig. 9 Mass loss of alkali activated specimens enhanced with mixed ratio of nano materials, **a** nano-glass and nano-kaolin, **b** nano-silica fume and nano-kaolin and fired up to 1000 °C

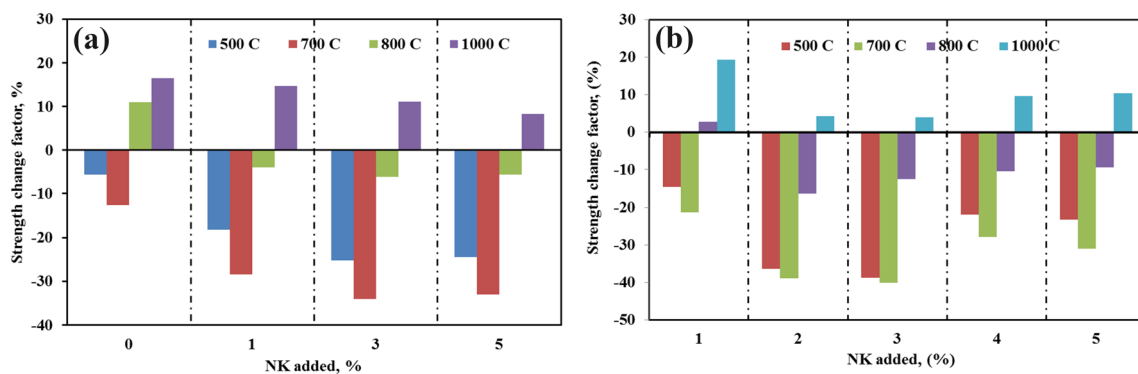


Fig. 10 Strength change factor of alkali activated specimens enhanced with mixed ratio of nano materials, **a** nano-glass and nano-kaolin, **b** nano-silica fume and nano-kaolin and fired up to 1000 °C

3.2 Effect of temperature on nano-materials enhanced geopolymer composite

3.2.1 Compressive strength examination

In comparison to the control mix, compressive strength for hardened alkali activated mixes having various ratios of nanomaterials powder burned from 500 to 1000 °C for 2 h with a heating rate of 5 °C/min is shown in Fig. 9. From the pattern, the strength of hardened pastes exposed to various temperatures grows up to 700 °C, and then decreases when fired at 800 °C and 1000 °C. Furthermore, strength varied according to the NK with respect to the other used nano; where replacing nano glass with 1% nano-kaolin results in improvement in the mechanical behavior which kept its performance up to 700 °C. Further increase in nano-kaolin results in the decrease in strength for all studied firing temperature. The same behavior was depicted for nano-silica fume which replaced by nano-kaolin where the enhancement observed up to 2% NK.

Dehydroxylation of kaolinite materials forms metakaolin, which may enrich the matrix with excess amorphous materials, resulting in the creation of three-dimensional geopolymer that can persist high firing temperatures up to 700 °C. However, increasing the temperature to 800 °C causes strength degradation, which could be due to dehydration and dehydroxylation of the geopolymer structure [48].

3.2.2 Strength change factor (SCF)

The strength change factor (SCF) of fired Nano-enhanced geopolymer composites fired up to 1000 °C is shown in Fig. 10. SCF is a measure of how much strength is lost or gained when fired at different temperatures. Negative SCF values in

concrete specimens without Nano-glass indicate an increase in compressive strength, which is most likely due to reaction product and crystallization salt filling holes. Several researchers have also reported on this phenomenon [49].

Except for those fired at 500 and 700 °C as well as some of those fired at 800 °C and activated with Nano-materials powder, the figure depicts the increase in positive SCF with increasing temperature up to 1000 °C. The figure also shows that the SCF grows with higher temperatures, particularly at 1000 °C, but it exhibits higher values at 1000 °C than at 800 °C, as expected from the compressive strength pattern, which will be related to the decreased strength at this temperature as compared with the control one.

On the other hand, firing at 500, 700 and 800 °C lead to increasing the strength as reflected on the negative value of SCF where the used kaolinite material transferred into metakaolin in addition to enhancing effect of added Nano-materials as well as the nucleation effect for geopolymer formation and accumulation, resulting in an increased formation of geopolymer chains.

The same pattern was observed for NK-NSF matrix, however the common phenomena is an increasing of SCF in the negative scale up to 500 °C and of little extent at 700 °C reflecting the low enhancement of NK for those mixes. The previous explanations can be related to microstructure of NK (less than 35–90 nm) and N-silica fume (coarse spherical nano particles 35–125 nm) while nano-glass is small nano-agglomerated particles that condense forming dense matrix and can withstand firing temperatures up to 700 °C with little strength gain at 800 °C.

3.2.3 Visual examination

A clear difference between samples was noted when visual evaluation was performed for fire hardened composites shot at various temperatures and incorporating varying NK from 0 to 5% for Nano-glass enhanced matrices (Fig. 11). All samples have a heat resistance of up to 700 °C while samples having 1% NK nearly free of voids as well as with no colour change up to 1000 °C. This is related to kaolinite's dehydroxylation as well as nanoparticles' activation. Most samples show evident damage at 800 °C, with their color shifting to a whiter form as a result of dehydration of CSH and binding phases within the matrix. On the other hand, most samples that are fired at 1000 °C encounter small cracks with etches at the edges specially at 0% NK with stable thermal cubes which may be due to metastable phases formation that resist high temperatures.

On the other hand visual images for NK from 0 to 4% for Nano-silica fume matrices (Fig. 12), All samples have a heat resistance of up to 700 °C while samples having 2% NK nearly free of voids as well as with no colour change up to 1000 °C. This is related to kaolinite's dehydroxylation as well as nanoparticles' activation. Most samples show evident damage at 800 °C, with their color shifting to a whiter form as a result of dehydration of CSH and binding phases within the matrix.

Fig. 11 Visual examination pattern of alkali activated specimens enhanced with various ratio of nano materials fired up to 1000°C

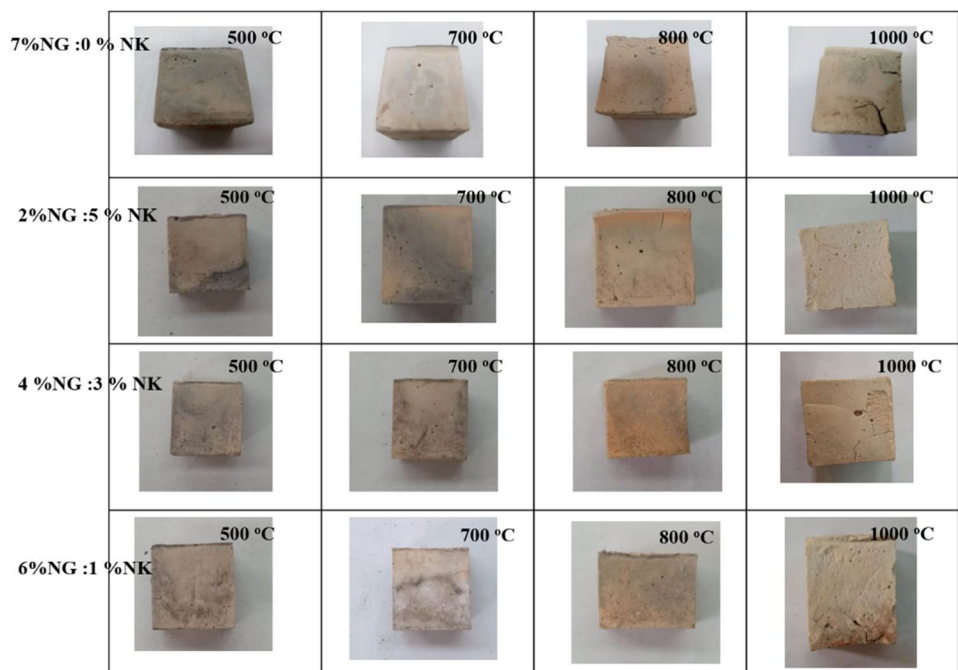
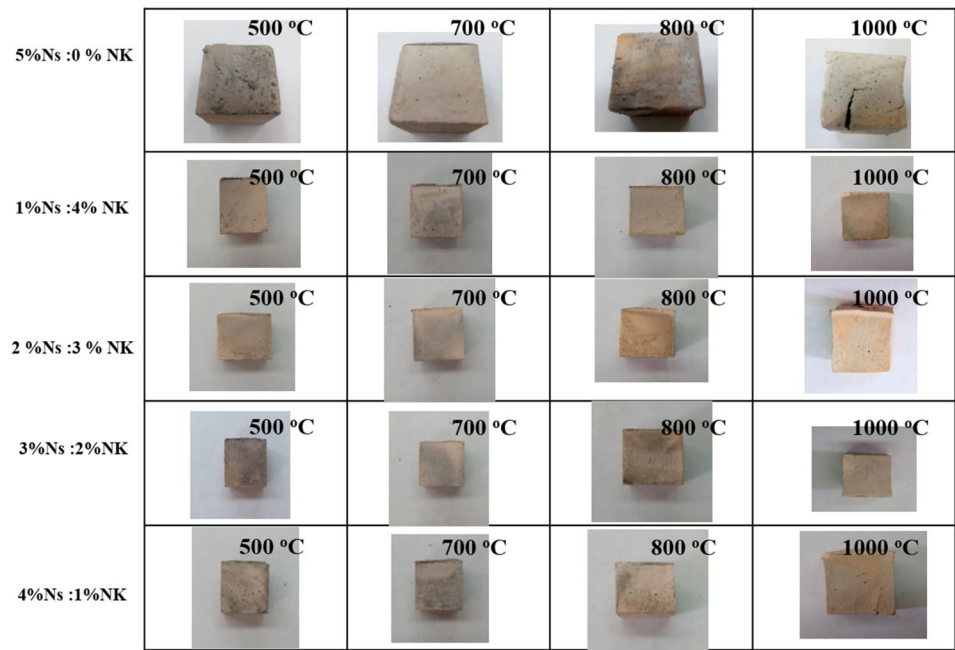


Fig. 12 SEM images of alkali activated specimens enhanced with mixed ratio of nano-materials of nano-silica fume and **a** 0, **b** 2, **c** 3% nano-kaolin



On the other hand, most samples that are fired at 1000 °C encounter small cracks with etches at the edges specially at 0% NK with stable thermal cubes which may be due to metastable phases formation that resist high temperatures.

4 Conclusions

After discussing and analyzing the results in detail in this article the main findings are summarized below:

1. It is possible to use the mixes containing limestone and nano materials to solve the problem of using heat curing, thermal energy consumption and pollution by reducing the MK used for MK-geopolymer cement.
2. Addition of NK to both Nano-glass and Nano-silica fume results in an enhancement in morphological and physico-mechanical characteristics of the formed geopolymer samples.
3. The enhancement and modification of the hardened geopolymer specimens achieved when using NK up to 1% for Nano-glass matrices and 2% for Nano-silica fume matrices.
4. DTG and TGA confirmed the enhancement effect of NK on both matrices (Nano-glass and Nano-silica fume).
5. Nano-glass mixes having 1% NK gives a strength values of about 55 MPa, Nano-silica fume mixes gives a strength of about 50 MPa after 90 days.
6. The hardened pastes has a positive tendency to resist the firing temperature up to 700 °C giving strength values of more than 65 MPa for 1%NK for Nano-glass matrices, while those of Nano-silica fume having 2% NK gives about 60 MPa.
7. Firing at 800 °C gives high strength values for both matrices reaching to 50 MPa.

Author contributions Dr. Hisham Khater: contribute for proposing the work of the paper, preparation of the materials, interpretation of the data, writing the manuscript as well as language editing. Dr. Mahmoud Ghariieb: contribute for proposing the work of the paper, preparation of the materials, interpretation of the data, writing the manuscript as well as language editing.

Funding Open access funding provided by The Science, Technology & Innovation Funding Authority (STDF) in cooperation with The Egyptian Knowledge Bank (EKB). The authors have not disclosed any funding.

Availability of data and materials All data generated or analyzed during this study are included in this published article and its supplementary information files.

Declarations

Ethics approval and consent to participate Not applicable.

Consent for publication Not applicable.

Competing interests The authors declare that they have no known competing financial interests or personal relationships that could have appeared to influence the paper.

Open Access This article is licensed under a Creative Commons Attribution 4.0 International License, which permits use, sharing, adaptation, distribution and reproduction in any medium or format, as long as you give appropriate credit to the original author(s) and the source, provide a link to the Creative Commons licence, and indicate if changes were made. The images or other third party material in this article are included in the article's Creative Commons licence, unless indicated otherwise in a credit line to the material. If material is not included in the article's Creative Commons licence and your intended use is not permitted by statutory regulation or exceeds the permitted use, you will need to obtain permission directly from the copyright holder. To view a copy of this licence, visit <http://creativecommons.org/licenses/by/4.0/>.

References

1. Bawab J, Khatib J, El-Hassan H, Assi L, Kirgiz MS. Properties of cement-based materials containing cathode-ray tube (CRT) glass waste as fine aggregates: a review. *Sustainability*. 2021;13(20):11529.
2. Katman HYB, Khai WJ, Bheel N, Kirgiz MS, Kumar A, Benjeddou O. Fabrication and characterization of cement-based hybrid concrete containing coir fiber for advancing concrete construction. *Buildings*. 2022;12(9):1450.
3. Kirgiz MS. Advancements in properties of cements containing pulverised fly ash and nanomaterials by blending and ultrasonication method (review-part II). *Nano Hybrids Comp*. 2019;24(12):37–44.
4. Balaguru P, Chong K. Nanotechnology and concrete: research opportunities. In: Balaguru P, Chong K, editors. *Proceedings of the ACI session on nanotechnology of concrete: recent developments and future perspectives*. Alexandria: National Science Foundation; 2006. p. 15–28.
5. Nasir M, Aziz MA, Zubair M, Manzar MS, Ashraf N, Mu'azu ND, Al-Harhi MA. Recent review on synthesis, evaluation, and SWOT analysis of nanostructured cellulose in construction applications. *J Build Eng*. 2022;46: 103747.
6. Shilar FA, Ganachari SV, Patil VB. Advancement of nano-based construction materials: a review. *Constr Build Mater*. 2022;359:129535.
7. Shilar FA, Ganachari SV, Patil VB. Investigation of the effect of granite waste powder as a binder for different molarity of geopolymer concrete on fresh and mechanical properties. *Mater Lett*. 2022;309:131302.
8. Khater HM. Calcium effect on geopolymerization of aluminosilicate wastes. *J Mater Civ Eng*. 2012;24(1):92–101.
9. Kuo WY, Huang JS, Lin CH. Effects of organo-modified montmorillonite on strengths and permeability of cement mortars. *Cem Concr Res*. 2006;36(5):886–95.
10. Li H, Xiao HG, Ou JP. A study on mechanical and pressure-sensitive properties of cement mortar with nanophase materials. *Cem Concr Res*. 2004;34(3):435–8.
11. Möschneret Li H, Zhang MH, Ou JP. Flexural fatigue performance of concrete containing nano-particles for pavement. *Int J Fatigue*. 2007;29(7):1292–301.
12. Khater HM. Effect of nano silica on microstructure formation of low cost geopolymer binder. *J Nanocomp*. 2016;2(2):84–97. <https://doi.org/10.1080/20550324.2016.1203515>.
13. Salami BA, Ibrahim M, Al-Osta MA, Nasir M, Ali MR, Bahraq AA, Wasia A. Engineered and green natural pozzolan-nano silica-based alkali-activated concrete: shrinkage characteristics and life cycle assessment. *Environ Sci Pollut Res*. 2023;30(7):17840–53.
14. Ibrahim M, Nasir M, Hussaini SR, Najamuddin SK, Ewebajo AO. Performance of structurally viable green concrete derived from natural Pozzolan and Nanosilica. *Mag Civ Eng*. 2021;107(7):2712–8172.
15. Khater HM, Abd el Gawwad HA. Synthesis and characterization of MK/Slag geopolymer composites enhanced by various ratios of nano kaolin. *Építőanyag*. 2017;69(2):40–8. <https://doi.org/10.14382/epitoanyag-jsbcm.2017.8>.
16. Buffat P, Borel JP. Size effect on the melting temperature of gold particles. *Phys Rev A*. 1976;13(6):2287.
17. Cyr M, Lawrence P, Ringot E. Efficiency of mineral admixtures in mortars: quantification of the physical and chemical effects of fine admixtures in relation with compressive strength. *Cem Concr Res*. 2006;36(2):264–77.
18. Dolado JS, Campillo I, Erkizia E, Ibanez JA, Porro A, Guerrero A, Goñi S. Effect of nanosilica additions on belite cement pastes held in sulfate solutions. *J Am Ceram Soc*. 2007;90(12):3973–6.
19. Li G. Properties of high-volume fly ash concrete incorporating nano-SiO₂. *Cem Concr Res*. 2004;34:1043–9.
20. Gaitero JJ, Campillo I, Mondal P, Shah SP. Small changes can make a great difference. *Transp Res Rec*. 2010;2141:1.
21. Seo JH, Kim DU, Nam JS, Hong SH, Sohn SB, Song SM. Radio frequency thermal plasma treatment for size reduction and spheroidization of glass powders used in ceramic electronic devices. *J Am Ceram*. 2007;90(6):1717–21.
22. Khater HM, El-Sabbagh BA, Fanny M, Ezzat M, Lottfy M. Effect of nano-silica on alkali activated water-cooled slag geopolymer. *ARPN J Sci Technol*. 2012;2(3):170–6.
23. Kakali G, Perraki T, Tsvivilis S, Badogiannis E. Thermal treatment of kaolin: the effect of mineralogy on the pozzolanic activity. *Appl Clay Sci*. 2001;20:73–80.

24. Wenying G, Guolin W, Jianda W, Ziyun W, Suhong Y. Preparation and performance of geopolymers. *J Wuhan Univ Technol Mater Sci Ed.* 2008;23(3):285–430.
25. Collins F, Lambert J, Duan WH. The influences of admixtures on the dispersion, workability, and strength of carbon nanotube–OPC paste mixtures. *Cement Concr Compos.* 2012;34(2):201–7.
26. Senff L, Hotza D, Repette WL, Ferreira VM, Labrincha JA. Effect of nanosilica and microsilica on microstructure and hardened properties of cement pastes and mortars. *Adv Appl Ceram.* 2010;109(2):104–10.
27. Shilar FA, Ganachari SV, Patil VB, Javed S, Khan TY, Baig RU. Assessment of destructive and nondestructive analysis for GGBS based geopolymer concrete and its statistical analysis. *Polymers.* 2022;14(15):3132.
28. Shilar FA, Ganachari SV, Patil VB, Khan TY, Javed S, Baig RU. Optimization of alkaline activator on the strength properties of geopolymer concrete. *Polymers.* 2022;14(12):2434.
29. Ouda AS, Gharieb M. Behavior of alkali-activated pozzocrete-fly ash paste modified with ceramic tile waste against elevated temperatures and seawater attacks. *Constr Build Mater.* 2021;285: 122866.
30. Rashad AM, Khafaga SA, Gharieb M. Valorization of fly ash as an additive for electric arc furnace slag geopolymer cement. *Constr Build Mater.* 2021;294: 123570.
31. Nasir M, Johari MAM, Maslehuddin M, Yusuf MO, Al-Harhi MA. Influence of heat curing period and temperature on the strength of silico-manganese fume-blast furnace slag-based alkali-activated mortar. *Constr Build Mater.* 2020;251: 118961.
32. ASTM C109M-12. Standard test method for compressive strength of hydraulic cement mortars. West Conshohocken: ASTM International; 2012.
33. Saikia N, Usami A, Kato S, Kojima T. Hydration behavior of ecocement in presence of metakaolin. *Resour Prog J.* 2004;51(1):35–41.
34. Khater HM. Influence of metakaolin on resistivity of cement mortar to magnesium chloride solution. *Ceram Silikáty J.* 2010;54(4):325–33.
35. Khater HM, Ghareib M. Utilization of alkaline aluminosilicate activation in heavy metals immobilization and producing dense hybrid composites. *Arab J Sci Eng.* 2021;46(7):6333–48.
36. Ugheoke BI, Onche EO, Namessan ON, Asikpo GA. Property optimization of kaolin-rice husk insulating fire-bricks. *Leon Electron J Pract Technol.* 2006;9:167–78.
37. Standards E. Concrete building units used in non-load and load bearing walls. Cairo: Egyptian Organization for Standardization; 1992. p. 1292.
38. Ganjian E, Pouya H. Effect of magnesium and sulfate ions on durability of silica fume blended mixes exposed to the seawater tidal zone. *Cem Concr Res.* 2005;35:1332–43.
39. Rashad AM, Gharieb M. Valorization of sugar beet waste as an additive for fly ash geopolymer cement cured at room temperature. *J Build Eng.* 2021;44: 102989.
40. Bernal S, De Gutierrez R, Delvasto S, Rodriguez E. Performance of an alkali-activated slag concrete reinforced with steel fibers. *Constr Build Mater.* 2010;24(2):208–14.
41. de Vargas AS, Dal Molin DC, Masuero AB, Vilela AC, Castro-Gomes J, de Gutierrez RM. Strength development of alkali-activated fly ash produced with combined NaOH and Ca (OH) 2 activators. *Cement Concr Comp.* 2014;53:341–9.
42. Gharieb M, Mosleh YA, Rashad AM. Properties and corrosion behaviour of applicable binary and ternary geopolymer blends. *Int J Sustain Eng.* 2021;14(5):1068–80.
43. Panias D, Giannopoulou IP, Perraki T. Effect of synthesis parameters on the mechanical properties of fly ash-based geopolymers. *Colloids Surf A Physicochem Eng Asp.* 2007;301:246–54.
44. Khater HM. Effect of silica fume on the characterization of the geopolymer materials. *Int J Adv Struct Eng.* 2013;5(12):1–10.
45. Duxson P, Lukey GC, van Deventer JS. Thermal evolution of metakaolin geopolymers: part 1—physical evolution. *J Non Cryst Solids.* 2006;352(52–54):5541–55.
46. Sivasakthi M, Jeyalakshmi R, Rajamane NP, Jose R. Thermal and structural micro analysis of micro silica blended fly ash based geopolymer composites. *J Non Cryst Solids.* 2018;499:117–30. <https://doi.org/10.1016/j.jnoncrsol.2018.07.027>.
47. Ismail I, Bernal SA, Provis JL, San Nicolas R, Brice DG, Kilcullen AR, Hamdan S, van Deventer JS. Influence of fly ash on the water and chloride permeability of alkali-activated slag mortars and concretes. *Constr Build Mater.* 2013;48:1187–201. <https://doi.org/10.1016/j.conbuilmat.2013.07.106>.
48. Temuujin J, Van Riessen A, Williams R. Influence of calcium compounds on the mechanical properties of fly ash geopolymer pastes. *J Hazard Mater.* 2009;167(1–3):82–8.
49. Khater HM, El Nagar AM. preparation of Sustainable eco-friendly MWCNT-geopolymer composites with superior sulfate resistance. *Adv Compos Hybrid Mater.* 2020;3:375–89. <https://doi.org/10.1007/s42114-020-00170-4>.
50. Khater HM. Nano-Silica effect on the physicomechanical properties of geopolymer composites. *Adv Nano Res.* 2016;3:1–14. <https://doi.org/10.12989/anr.2016.4.5.181>.
51. Khater HM, Zedane SR. Geopolymerization of industrial by-products and study of their stability upon firing treatment. *Int J Eng Technol.* 2012;2(2):308–16.
52. Gomes S, Petit E, Frezet L, Thirouard R, Taviot-Gueho C, Gharzouni A, Rossignol S, Renaudin G. Temperature stability of a pure metakaolin based K-geopolymer: part 1. Variations in the amorphous mineral network. *J Am Ceram Soc.* 2020;103(10):5914–26.